Hung et al., http://www.jcb.org/cgi/content/full/jcb.201302132/DC1

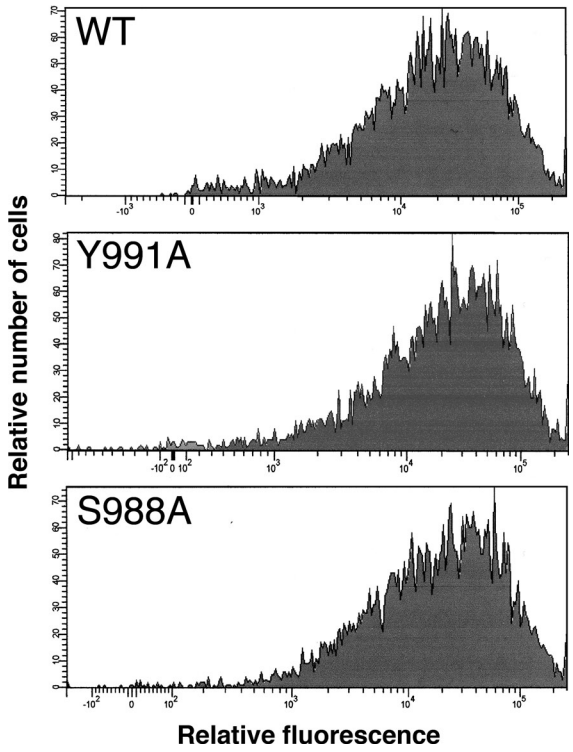

Figure S1. **Surface expression of α4 integrin in CHO-α4WT, CHO-α4Y991A, and CHO-α4S988A cells.** Cells were analyzed by flow cytometry using an anti–α4 integrin antibody (clone P1H4 obtained from EMD Millipore) and a goat anti–mouse allophycocyanin-conjugated secondary antibody (Santa Cruz Biotechnology, Inc.). Note that the surface expression of α4 integrin is similar in all three cell types.

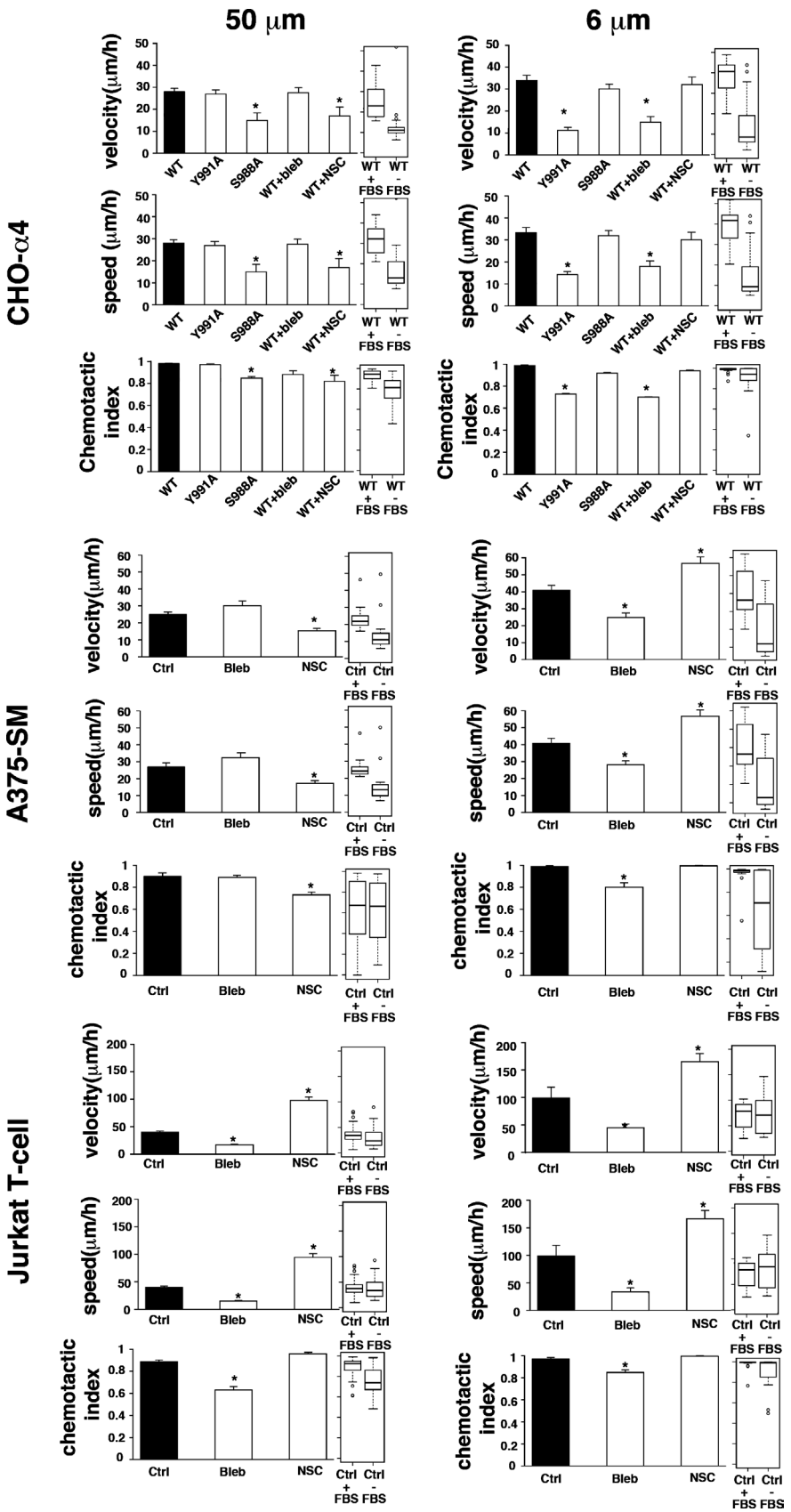

Figure S2. **Quantitative analysis of velocity, speed, and chemotactic index of α4 integrin–expressing CHO, A375-SM, and Jurkat T cells in wide and narrow channels.** Cell motility was evaluated by analyzing three parameters: (1) velocity (net cell displacement per unit time), (2) speed (total migration path per unit time), and (3) chemotactic index (net cell displacement divided by total path). Data represent means ± SEM of ≥40 cells from three independent experiments. *, $P < 0.005$. The presence or absence of FBS on cell migration in wide and narrow channels is also presented in a box plot, demonstrating first, second, third quartiles, variance, and outliers. Data represents ≥25 cells. Ctrl, control; Bleb, blebbistatin; NSC, NSC23766.

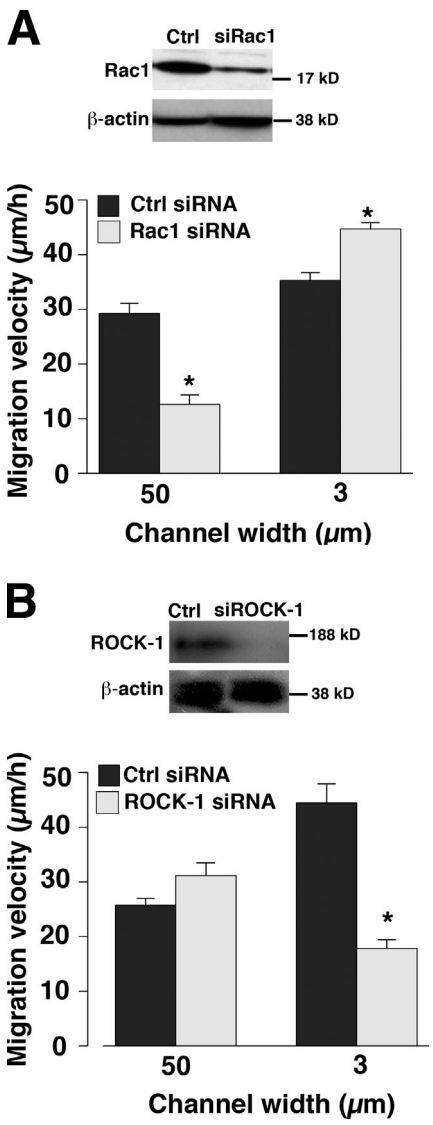

Figure S3. **Effects of Rac1 and ROCK-1 depletion on the migration of CHO-α4WT cells.** (A and B) CHO-α4WT cells were transfected with 30 nM Rac1 siRNA (A), 200 nM ROCK-1 siRNA (B), or control siRNA (Ctrl) at the corresponding concentrations. The depletion of Rac1 and ROCK-1 was demonstrated by immunoblotting using an anti-Rac1 and anti–ROCK-1 antibody, respectively. β-Actin served as an internal control. The migration velocity of Rac1-, ROCK-1–depleted, or control CHO-α4WT cells inside 50- and 3-μm channels was quantified. Data represent means ± SEM of >45 cells from three independent experiments. *, $P < 0.005$ relative to a control siRNA.

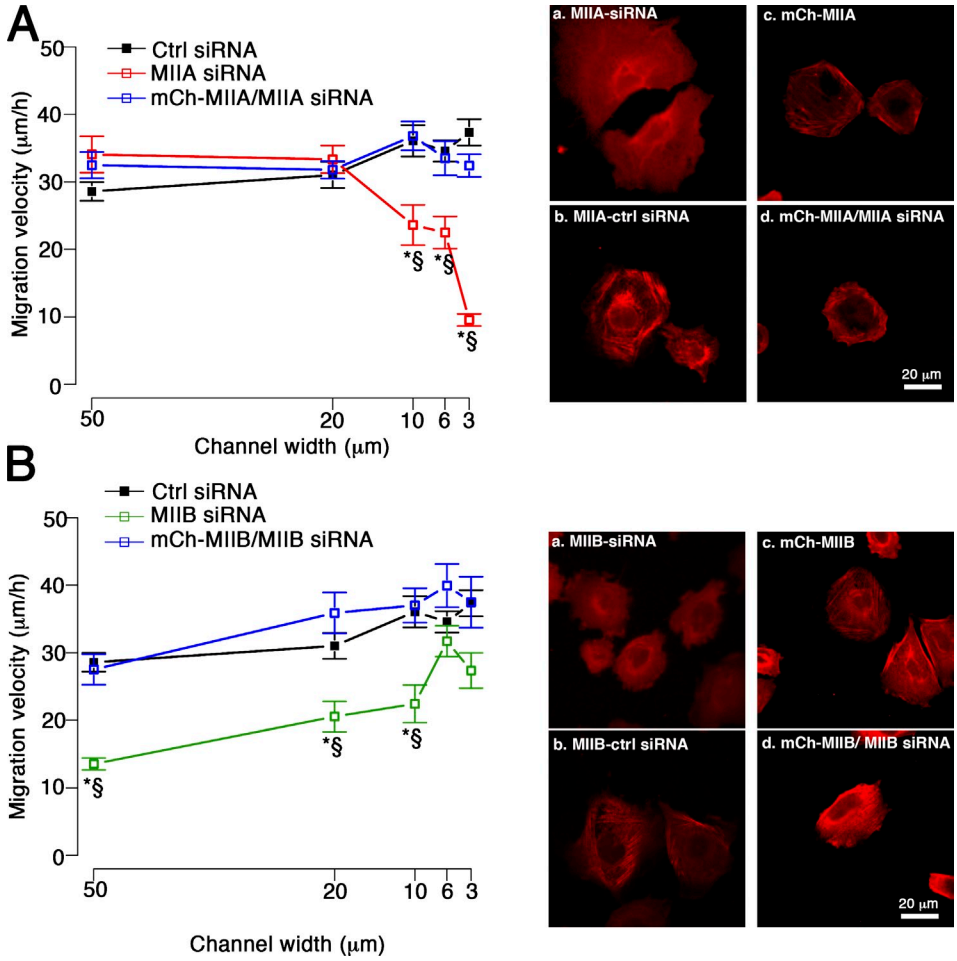

Figure S4. **Rescue of migration defect of MIIA or MIIB depletion by cotransfection with mCherry-MIIA or mCherry-MIIB in CHO-α4WT cells.** (A) Cells were transfected with either 60 nM MIIA siRNA or scramble control (Ctrl) or cotransfected with 1 ng/ml MIIA siRNA and 60 nM mCherry (mCh)-MIIA. (B) Similarly, cells were transfected with 60 nM MIIB siRNA or scramble control or cotransfected with 1 ng/ml MIIA siRNA and 60 nM mCherry-MIIB. The depletion and rescue of MIIA and MIIB were confirmed by the absence or presence of stress fibers visualized by immunofluorescent staining with antibodies against MIIA (A, a and b) or MIIB (B, a and b), or by the fluorescence of mCherry (A, c and d, for MIIA; and B, c and d, for MIIB). The migration velocity of MIIA- and MIIB-depleted, MIIA and MIIB-rescued, or scramble control CHO-α4WT cells inside microchannels of different widths was quantified. Data represent means ± SEM of >25 cells from at least two independent experiments. *, $P < 0.005$ relative to a control siRNA. §, $P < 0.005$ relative to mCherry-MIIA/siRNA MIIA or mCherry-MIIB/siRNA MIIB.

A

	WT		Y991A		S988A	
	W	N	W	N	W	N
untreated	+++	+++	+++	+	+	+++
NSC23766	+	+++	+	+++	+	+++
Y-27632	+++	+	+++	+	+++	+
Blebb	+++	+	+++	+	+++	+

	WT	
	W	N
untreated	+++	+++
ML-7	+	+
Y-27632	+++	+
Blebb	+++	+
MIIA-KD	+++	+
MIIB-KD	+	+++

B

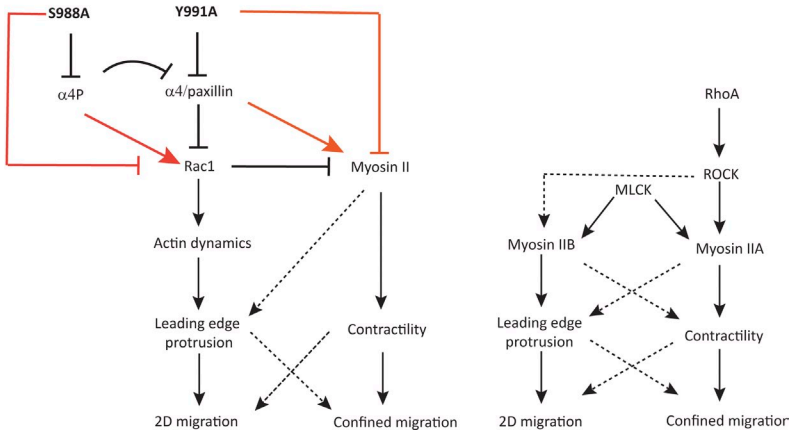

Figure S5. **Model and summary of α4 tail–mediated signaling in optimizing 2D and confined migration.** (A) The tables summarize the effects of introducing the α4 tail mutations or various pharmacological inhibitors/siRNAs on the migration of α4 integrin–expressing CHO cells through wide (W) and narrow (N) channels. The single plus signs correspond to low migration velocity. In contrast, the triple plus signs correspond to high migration velocity. (B) Distinct signaling pathways regulate 2D versus confined migration. Black lines, primary pathway; orange lines, end result from several signaling steps; black dashed lines, involved but not required. Blebb, blebbistatin.

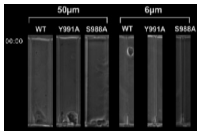

Video 1. **Migration of CHO-α4WT, CHO-α4Y991A, and CHO-α4S988A cells through 50- and 6-µm channels.** Images were acquired by time-lapse microscopy using an inverted microscope (Eclipse Ti). Frames were taken every 10 min for 8 h. The video accompanies Fig. 2 B. Time shows hours and minutes.

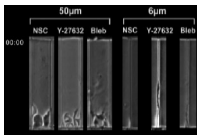

Video 2. **Migration of NSC23766-, Y-27632–, or blebbistatin-treated CHO-α4WT cells through 50- and 6-µm channels.** After 1-h incubation of CHO-α4WT cells with the indicated inhibitor or vehicle control at 37°C, 10% FBS was added to the topmost (chemotactic) inlet port to induce migration. Images were acquired by time-lapse microscopy using an inverted microscope (Eclipse Ti). Frames were taken every 20 min for 8 h. The video accompanies Fig. 3 A. Time shows hours and minutes. Bleb, blebbistatin; NSC, NSC23766.

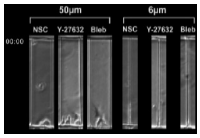

Video 3. **Migration of NSC23766-, Y-27632–, or blebbistatin-treated CHO-α4Y991A cells through 50- and 6-µm channels.** After 1-h incubation of CHO-α4Y991A cells with the indicated inhibitor at 37°C, 10% FBS was added to the topmost (chemotactic) inlet port to induce migration. Images were acquired by time-lapse microscopy using an inverted microscope (Eclipse Ti). Frames were taken every 20 min for 8 h. The video accompanies Fig. 3 B. Time shows hours and minutes. Bleb, blebbistatin; NSC, NSC23766.

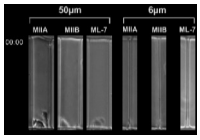

Video 4. **Migration of MIIA-depleted, MIIB-depleted, or ML-7–treated CHO-α4WT through 50- and 6-µm channels.** Migration of CHO-α4WT cells transfected with MIIA or MIIB siRNA or treated with 25 µM ML-7 was induced by chemoattractant (10% FBS). Images were acquired by time-lapse microscopy using an inverted microscope (Eclipse Ti). Frames were taken every 10 min for 8 h. Time shows hours and minutes. The video accompanies Fig. 7 (B and C).